Accessing a Diverse Set of Functional Red-Light Photoswitches by Selective Copper-Catalyzed Indigo *N*-Arylation

Amit K. Jaiswal, Priya Saha, Julong Jiang, Kimichi Suzuki, Anna Jasny, Bernd M. Schmidt, Satoshi Maeda,* Stefan Hecht,* Chung-Yang (Dennis) Huang*

ABSTRACT: The ability to correlate the structure of a molecule to its properties is the key to a rational and accelerated design of new functional compounds and materials. Taking photoswitches as an example, the thermal stability of meta-stable state is a crucial property that dictates their application in molecular systems. Indigos have recently emerged as an attractive motif for designing photoswitchable molecules due to their red-light addressability, which can be advantageous in biomedical and material applications. The absence of comprehensive synthetic techniques and a thorough understanding of the impact of structural factors on the photochemical and thermal properties of this widely available dye hinders its broad application. Herein, we report an efficient copper-catalyzed indigo *N*-arylation that enables the installation of a wide variety of aryl moieties carrying useful functional groups. The exclusive selectivity for mono-arylation likely originates from a bimetallic cooperative mechanism through a binuclear copper-indigo intermediate. Functional *N*-aryl-*N*′-alkylindigos were prepared and shown to photoisomerize efficiently under red light. Moreover, this design allows for the modulation of thermal half-lives through *N*-aryl substituents, while the *N*′-alkyl groups enable the independent attachment of functional moieties without affecting the photochromic properties. Strong correlation between the structure of *N*-aryl moiety and the thermal stability of the photogenerated *Z*-isomers was achieved by multivariate linear regression models obtained through a straightforward data-science workflow. This work thus builds an avenue leading to versatile red-light photoswitches and a general method for structure-property correlation that is expected to be broadly applicable to the design of photoresponsive molecules.

INTRODUCTION

Introducing photocontrol with high spatial, temporal, and spectral resolution has become an attractive strategy to build advanced functions into molecular systems. By incorporating an effective mediator, the light-energy can be directed to modulate the targeted physical, chemical, and biological properties of the system. Among all mediators, photoswitches, molecules that undergo reversible light-induced structural changes, have emerged as popular candidates across numerous scientific fields.[1] For example, azobenzenes and diarylethenes are the two most widely used classes of photoswitches, where the steric or electronic changes upon either E/Z isomerization or electrocyclization can be exploited in designing photoresponsive systems for various applications.

Two characteristics are crucial for implementing photoswitches in molecular systems. First, the absorption wavelength, typically at its maximum (λ_{max}), determines the light energy required to induce the photoisomerization process. Eyeing on applications in biomedicine[2] and material science[3], recent attention has shifted to photochromic moieties that can be operated using visible and, more preferably, red and near-infrared (NIR) light.[4] These long-wavelength photons possess less energy and thus a lower propensity to cause damage while at the same time, displaying superior penetration through tissue and thus living organisms.[5] Second, the stability of the switched state, as denoted by the thermal half-life of the meta-stable isomer or the rate of the thermal back-reaction, dictates how long the photogenerated form remains active or inactive depending on the type of system, i.e. OFF→ON and ON→OFF, respectively. Ideally, the thermal stability can be tuned within a wide range to match the particular kinetics dictated by the chosen design.

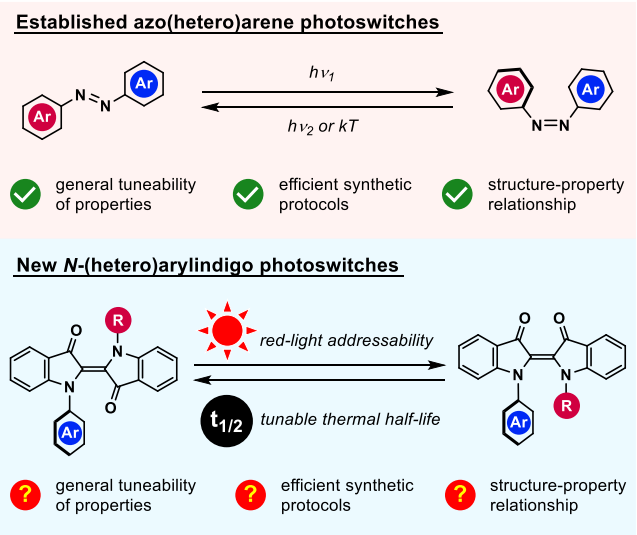

Figure 1. Development of new *N*-arylindigos as red-light photoswitches.

Indigo is one of the most ancient and abundant dyes utilized in our daily lives, most notably in denim for blue jeans.[6] As opposed to many dye molecules that require extended π-systems to even reach visible-light

absorption, this blue dye of small molecular structure absorbs naturally in the red-light region, thanks to its two push-pull, nitrogen/carbonyl pairs around the central double bond. Since the 1950's, it has been known that *N,N´*-disubstituted indigos can undergo red-light-induced *E*/*Z* isomerization.[7] Recently, interest in utilizing the photochromic properties of indigos has been rekindled because of their multifaceted merits. Indigo photoswitches can function as superior geometrical switches when compared to azobenzenes due to their ~180° rotation during *E*/*Z* isomerization. In addition, indigos are negative photochromic molecules, which means that upon irradiation, the spectra become hypsochromically shifted.[8] In combination with their intense absorption in the red region of the spectrum associated with the biological window, this feature has significant implications in biomedical applications, as it allows to penetrate human tissue depth over time. Their red/NIR addressability has made indigos an emerging class of photoswitches for biomedical applications. In this context, their non-toxic nature proves advantageous as well.[9] Last but certainly not least, the availability of synthetic methods to prepare a wide variety of indigo derivatives from readily available and inexpensive dyestuffs will facilitate their exploration and ultimate use.

Although the parent indigo does not undergo photoisomerization due to competing excited-state proton transfer (ESPT),[10] its derivatives carrying substituents on either one or both nitrogen atoms function as efficient photoswitches. As a result, the *N*-substituents play a crucial role in modulating the photochemical properties of indigos. Most of the studied indigo photoswitches possess either *N*-acyl or *N*-alkyl substituents.[6] However, whereas *N*-acyl groups shift the absorption too far to the blue region of the spectrum, i.e. away from the biological window, *N*-alkyl groups lead to extremely short thermal half-lives of the photogenerated *Z*-isomer.

In 2017, we reported on *N*-arylindigos and demonstrated that upon proper *N*-aryl substitution, the thermal stability of the corresponding *Z*-isomers can be tuned while maintaining their absorption in the red region of the spectrum.[11] We found that the rates of the thermal back-reaction are directly correlated with the electronic properties of the *N*-aryl groups, where electron-withdrawing arenes result in slower reactions, i.e., longer thermal half-lives. We also showed that this important electronic effect of *N*-aryl substituents originates from their perpendicular geometry to the indigo plane, which allows them to modulate the chromophore through inductive rather than resonance effects (as opposed to *N*-acyl groups).[12]

For these reasons, we have engaged to incorporate *N*-arylindigos in functional materials.[13] However, one of the remaining obstacles relates to the lack of efficient synthetic methodologies to prepare these structural motifs in an efficient and flexible manner (Figure 1). Direct *N*-arylation of indigo has been reported, albeit in unbearably low yields and/or requiring harsh conditions.[11,14] Consequently, on the one hand, *N*-aryl moieties with functional groups for selective and mild post-functionalization could not be included. On the other hand, the selectivity for mono-arylation can sometimes be low under forcing reaction conditions, generating at the same time bis-arylated products along with an array of side products. To overcome this challenge, we sought to identify a suitable catalytic system that would enable efficient and selective indigo *N*-arylation. Here we report our development of a copper-catalyzed protocol for the installation of key indigo *N*-aryl groups leading to a collection of attractive functional red-light photoswitches. Furthermore, the construction of multivariate linear regression models allows for the correlation between their molecular structures and the rates of thermal back-reaction.

Table 1. Screening of Cu-catalyzed indigo *N*-arylation conditions

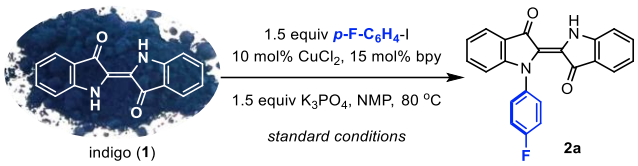

entry	variables	conditions	yield[a]
1	ligand[b]	2,2'-bipyridine (bpy)	77%
2		diamine	63%
3		diketone	30%
4		BPMO	55%
5	base[c]	K_3PO_4	77%
6		Cs_2CO_3 or CsF	50%
7		Na_2CO_3, K_2CO_3, or KOAc	<5%
8	solvent[d]	toluene, dioxane, DME, or DCE	<50%
9		DMA, DMF, DMSO, or pyridine	62-79%
10		NMP	84%
11	equiv[e]	bpy=0.30, K_3PO_4=3.0, ArI=3.0	82%
12		bpy=0.15, K_3PO_4=1.5, ArI=1.5	77%
13	ArBr or ArOTf instead of ArI		<5%
14	25-40 °C instead of 80 °C		<5%

[a]Isolated yields or LC yields using indigo carmine as standard; see SI for more optimizations; Ar = *p*-F-C_6H_4. [b]10 mol% CuI, 30 mol% **ligand**, 3.0 equiv K_3PO_4, 3.0 equiv ArI, pyridine (0.10 M), 80 °C. [c]10 mol% CuI, 30 mol% bpy, 3.0 equiv **base,** 3.0 equiv ArI, pyridine (0.10 M), 80 °C. [d]10 mol% CuI, 30 mol% bpy, 3.0 equiv K_3PO_4, 3.0 equiv ArI, **solvent** (0.10 M), 80 °C. [e]10 mol% $CuCl_2$, **bpy/K_3PO_4/ArI (equiv)**, NMP (0.10 M), 80 °C.

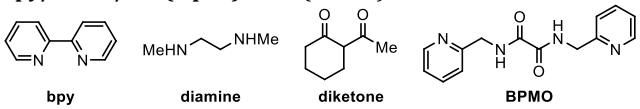

RESULTS AND DISCUSSIONS

Synthetic Protocol. We commenced our synthetic exploration by evaluating various transition metal catalysts able to forge the C–N bond with the parent indigo dye. The predominant choices for amination catalysts include Pd (Buchwald-Hartwig) and Cu (Ullmann-Goldberg) complexes.[15] We presumed that Cu-based catalysts would be more effective than the Pd variant, as the former in general favor electron-poor amines and amides, which more appropriately describes the nature of indigo nitrogen atoms as they are in conjugation with carbonyl groups. Indeed, while the Pd catalysts in combination with various classical ligand classes were ineffective, by switching to Cu catalysts, the desired mono-arylated product **2a** was obtained when an aryl iodide was used as the coupling partner (Table 1). Furthermore, ligand screening revealed that 2,2'-bipyridine-type ligands are most effective (entries 1–4), and we chose the most inexpensive 2,2'-bipyridine (bpy) for further optimization. Bases play a crucial role in this protocol, and K_3PO_4 was found to afford the highest yield (entries 5–7). On the other hand, the low solubility of the indigo dye requires a sufficiently polar solvent for high yields (entries 8–10). By employing these parameters, we further reduced the loadings of the ligand, the base, and the aryl iodide to arrive at a more economical and scalable protocol without much compromise in yields (entries 11 and 12). As a result, using these conditions involving solely inexpensive and commercially available reagents, the desired *N*-arylindigo (**2a**) could be obtained in 77% yield. Note that when aryl bromides or triflates were used as the coupling partner, only trace amounts of arylated product were observed, presumably due to a less facile oxidative addition to the Cu-catalyst as compared to aryl iodides (entry 13). Attempts to lower the reaction temperature resulted in diminished reactivities (entry 14).

Synthetic Scope. With the optimized conditions in hand, the reaction scope was subsequently examined (Scheme 1). Both electron-withdrawing (**2a**, **2e**, **2h**, **2j**) and -donating (**2b**, **2l**, **2o**) aryl groups can be tolerated, as well as heterocyclic substituents (**2c, 2d**, **2p**, **2t**). Gratifyingly, the utility of this method could be demonstrated by the successful inclusion of further derivatizable functional entities, such as halide (**2g**, **2m**), ester (**2i**), aldehyde (**2n**), olefin (**2q**), and alkyne (**2s**) groups. Aiming to show compatibility with complex molecule synthesis for biomedical applications, loratadine, an anti-allergic agent, was successfully coupled to indigo (**2u**). Overall, under these mild conditions, a wide variety of indigos functionalized with synthetically attractive motifs can be constructed. One limitation of this protocol relates to the low reactivity found for *ortho*-substituted aryl substrates (see SI for details).

Isolating the visually apparent blue band during column chromatography typically yielded analytically pure product in an operationally simple protocol (see SI for details). To further demonstrate the practicality of our method, we performed a gram-scale reaction to afford the *p*-bromophenyl derivative (**2v**) in 79% yield (Scheme 2). Moreover, we could exploit the orthogonal reactivity between Cu- and Pd-catalysis to perform a subsequent Suzuki-Miyaura coupling to prepare an elongated indigo derivative (**2w**).

Scheme 1. Reaction scope of Cu-catalyzed indigo *N*-arylation[a]

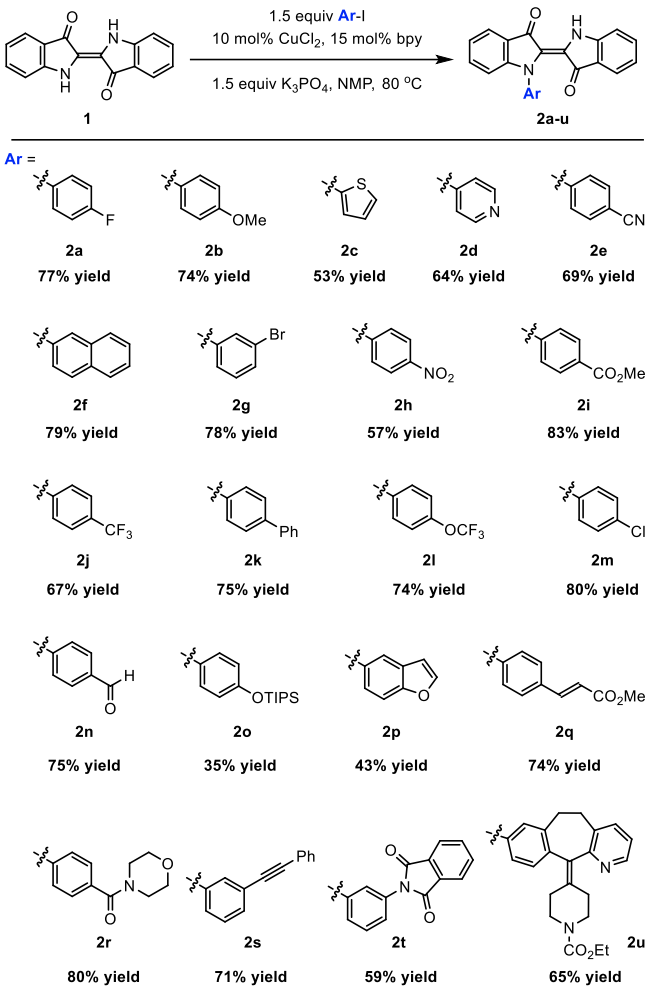

[a]Yields are the average of two runs, 0.50 mmol scale.

Scheme 2. Gram-scale reaction of indigo *N*-arylation and subsequent Suzuki-Miyaura derivatization

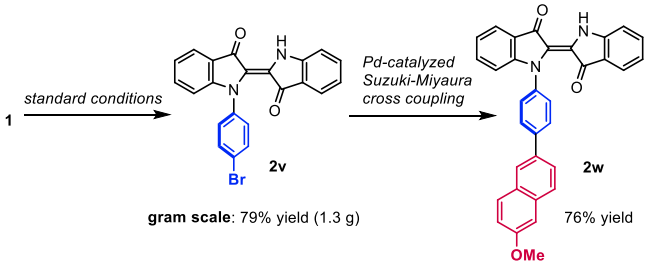

Mechanistic Considerations. An outstanding feature of our method is its surprising selectivity: Despite the presence of a second available *N*-nucleophile in the indigo core, only mono-arylated products were isolated to afford a clean reaction profile, even when using large excess of aryl halides. As reported in previous indigo *N*-

Scheme 3. Computed energy landscape of copper-catalyzed indigo *N*-arylation suggesting a minimum energy path via a bimetallic cooperative mechanism in the first *N*-arylation only[a]

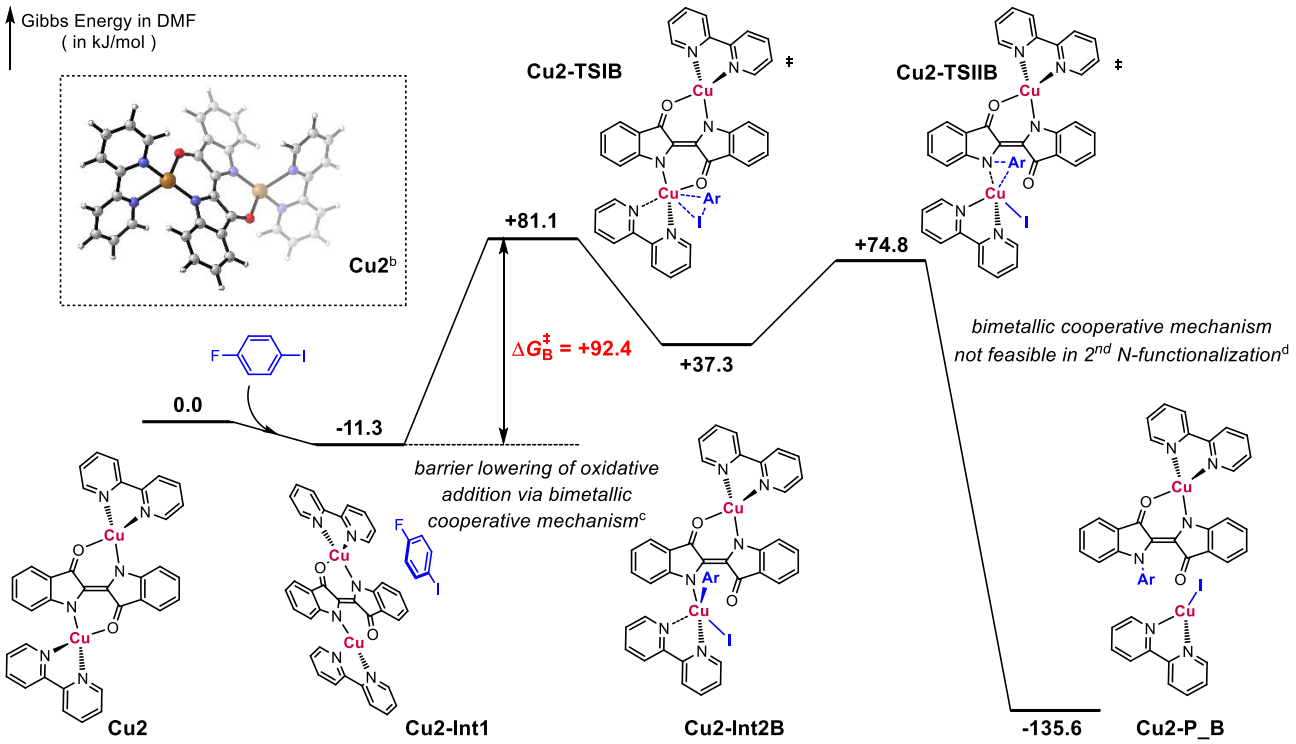

[a]Computed at DFT level of theory (B3LYP-D3/6-311G(d,p)//B3LYP-D3/6-311G(d,p), SDD basis sets used for Cu and I) with the implicit IEF-PCM solvation model (solvent = DMF). [b]Optimized geometry of **Cu2** shown in top left. [c]Barriers of 111.3 or 114.1 kJ/mol were obtained for the non-cooperative pathway (see Figure S10 for details). [d]Barriers were computed to be 112.6 or 122.3 kJ/mol for the second *N*-arylation (see Figure S11 for details).

arylation reactions under Ullmann-Goldberg conditions, double arylation was only observed under extremely forcing conditions.[14] To gain additional insights into the origin of this selectivity, we decided to take advantage of computational modelling.

By using *p*-fluoroiodobenzene as the model electrophile, DFT (density-functional theory) calculations at B3LYP-D3/6-311G(d,p) level of theory (while SDD pseudo-potential basis sets were used for Cu and I) were performed to explore the energy levels of potentially relevant intermediates and transition states along the reaction paths. In all cases, the oxidative addition of a copper-indigo complex to the aryl iodide was identified as the step with the highest activation barrier.[16,17] After testing various mechanistic scenarios *in silico*, we discovered that a binuclear Cu-indigo species (**Cu2**) effectively lowers the free energy barrier of the first oxidative addition to the level of 92.4 kJ/mol. Once the first N–H has been arylated, the second *N*-arylation, where the bimetallic structure is not feasible, was found to have an elevated barrier of 112.6 kJ/mol(Scheme 3).[18] This significant difference in energy would explain the reactivity differentiation for the two *N*-arylation steps. Electronic coupling between the two copper centers through the indigo core indeed seems to be the key in this bimetallic cooperative mechanism, in which the equilibrium between Cu(III)/Cu(I) and Cu(II)/Cu(II) configurations can help alleviate the barrier resulting from a high oxidation state copper (**Cu2-TSIB**).[19] Experimentally, the presence of **Cu2** is supported by its observation in mass spectrometry (see SI for details). Further investigation of the binuclear copper-indigo complexes as well as the application of bimetallic cooperative catalysis in indigo functionalization is currently underway. Moreover, this mechanism explains the failure of aryl bromides and triflates as coupling partners due to their excessive activation barriers for oxidative addition (see SI for details).

Photochromic Properties. Next, we proceeded to study the influence of these *N*-aryl groups on the photochromic properties. In order to be able to nicely compare all the compounds, we first alkylated the mono-*N*-arylindigos (**2a-u**) using a previously developed protocol to obtain *N*-aryl-*N´*-alkylindigos (**3a-u**) (Figure 2a).[11] The photoisomerization behavior of these molecules was then studied in MeCN and toluene upon illumination with a red-LED (660 nm, 20 nm full width at half-maximum). All compounds could be photoswitched with moderate to excellent efficiency in both solvents, as judged by the composition (Z-content) of the photostationary state (PSS), typically amounting to 40–70% in MeCN and 50–80% in toluene (Scheme 4). The photochromism is also visible to the naked eye with a color change from a blue to a purple PSS solution as a consequence of the 50–70 nm difference between the absorption maxima (λ_{max}) of the *E*- and *Z*-isomers (Figure 2b). Analysis of the structure of the selected derivative **3j** reconfirmed the perpendicular geometry of the *N*-aryl

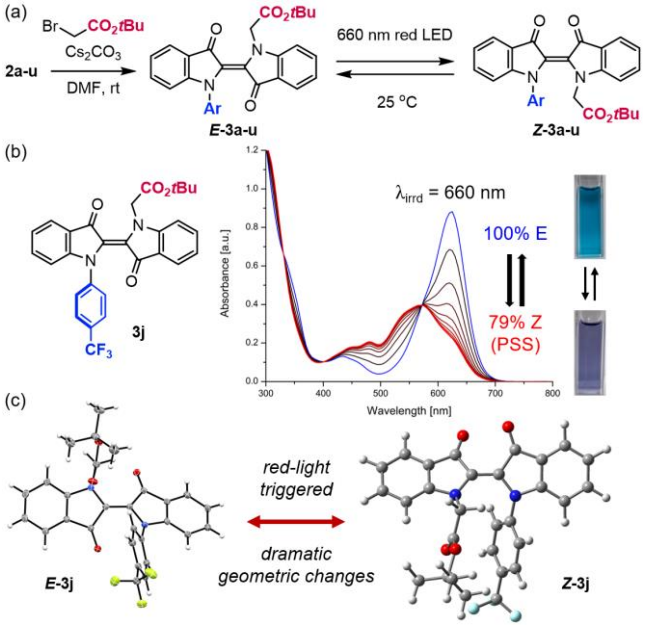

Figure 2. (a) Preparation of *N*-aryl-*N*′-alkylindigo photoswitches, (b) UV-vis spectrum and the color change in the photochromic study of indigo **3j** (a 5.8×10^{-5} M solution in toluene irradiated with 660 nm LED with spectra recorded every 30 s at 25°C), (c) X-ray structures of indigo ***E*-3j** and a DFT-computed structure of ***Z*-3j**.

groups relative to the indigo plane (Figure 2c) as well as the precursor **2j** (see SI). Comparison between the structures of ***E*-3j** (X-ray) and ***Z*-3j** (computed) reveals that upon photoisomerization, the relative spatial arrangement of the two *N*-substituents changes dramatically.

Importantly, despite the significant variations in *Z*-isomer thermal stability, the absorption maxima of the *E*-isomers remain relatively unaffected (λ_{max} = 616-631 nm), and there is only a very weak correlation between $t_{1/2}$ and λ_{max} (Scheme 4). Practically, all compounds regardless of their thermal half-lives could be efficiently switched using the same red LED (660 nm). Therefore, these *N*-aryl substituents serve as key modulators for indigo photoswitches with variable thermal half-lives while maintaining their advantageous red-light addressability. This character is in stark contrast to *N*-acyl or *N*-Boc-indigos, where their λ_{max} and $t_{1/2}$ are inevitably coupled, and consequently the red-light addressability is lost. Note that compounds with higher thermal stability of their *Z*-isomer also tend to afford higher *Z* content in their PSS, reflecting the fact that under current irradiation conditions, the kinetics of the thermal back-reaction have a significant influence on the photothermal-equilibrium.

These novel compounds thus represent a new design strategy for indigo photoswitches: By utilizing a single *N*-aryl substituent to control the thermal half-lives, the *N*′-alkyl group remains available to independently attach functional moieties without affecting their photochromic properties. To illustrate this concept, we prepared compound **4a**, which contains an alkyne for further conjugation through click chemistry. Copper-catalyzed azide-

Scheme 4. Photochromic and thermal behavior of indigo photoswitches 3a–u in MeCN and toluene: (a) Overview plot and (b) tabulated data.

(a)

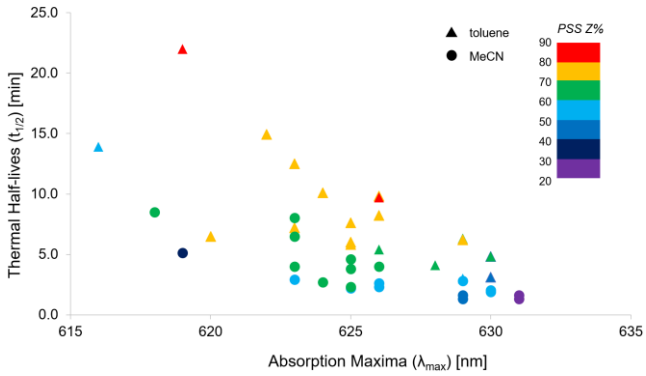

(b)

Compound[a]	$\lambda_{max,E}$ (nm)	$\lambda_{max,Z}$ (nm)	$t_{1/2}$ (min)	PSS Z%[b]
3a	625	575	2.2	58%
	625	**562**	**6.0**	**76%**
3b	631	580	1.3	25%
	630	**568**	**3.1**	**35%**
3c	619	569	5.1	34%
	616	**559**	**13.9**	**56%**
3d	618	567	8.5	68%
	619	**551**	**22.0**	**81%**
3e	623	569	6.5	66%
	623	**555**	**12.5**	**78%**
3f	630	575	2.0	52%
	629	**566**	**6.2**	**71%**
3g	623	573	2.9	59%
	620	**564**	**6.5**	**74%**
3h	623	570	8.0	69%
	622	**551**	**14.9**	**78%**
3i	626	572	4.0	62%
	626	**562**	**9.8**	**75%**
3j	623	570	4.0	63%
	624	**554**	**10.1**	**79%**
3k	626	574	2.6	58%
	625	**560**	**7.6**	**77%**
3l	629	577	2.8	53%
	629	**565**	**6.3**	**65%**
3m	630	580	1.9	50%
	630	**568**	**4.8**	**63%**
3n	625	572	4.6	62%
	626	**556**	**8.2**	**72%**
3o	624	570	2.7	61%
	623	**556**	**7.2**	**78%**
3p	629	584	1.3	45%
	628	**566**	**4.1**	**69%**
3q	631	580	1.6	28%
	630	**570**	**4.8**	**39%**
3r	626	574	2.3	55%
	626	**563**	**5.4**	**67%**
3s	625	571	2.3	60%
	625	**562**	**5.8**	**76%**
3t	625	570	3.8	64%
	626	**564**	**9.7**	**82%**
3u	629	576	1.6	47%
	629	**570**	**3.0**	**53%**

[a]Experiments were carried out by irradiating $4.0 \sim 5.0 \times 10^{-5}$ M solutions with 660 nm LED. Bold numbers in the bottom half of the rows are results obtained in toluene, whereas the top half are in MeCN. [b]Content of *Z*-isomers in photostationary state (PSS).

alkyne cycloaddition (CuAAC)[20] was used to introduce three different molecules bearing biologically relevant components to afford the desired compounds, as confirmed by mass spectrometry (see SI for details). To mimic the real application case, where the desired indigo photoswitches would be generated and isomerized *in situ*, we directly irradiated the diluted reaction mixture with a red LED. With this procedure, photoswitching was observed and, more to our delight, all three compounds despite having drastically different structures of the attached functional moieties, their indigo cores display nearly identical λ_{max} and thermal half-lives (Scheme 5). The switching efficiency was modest, presumably due to the remaining components in the mixture that could interfere with the photochemistry, but these preliminary experiments nicely demonstrate our *N*-aryl- *N'*-alkylindigos as photoswitches that enable red-light operation while allowing for thermal half-life modulation and covalent attachment to the target entity of choice.

Scheme 5. Attachment of functional moieties through CuAAC and the photochromic properties of 4b–4d and 4a (pure and in reaction mixture) measured in MeCN.

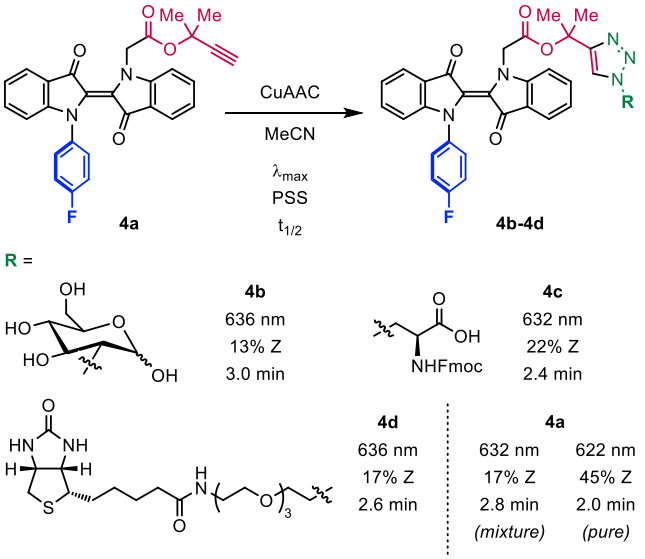

Multivariate Linear Regression Modeling. Given the impact of *N*-aryl substituents on the thermal half-lives of *Z*-isomers, we have been aiming to develop a quantitative model for correlating indigo structures with the rate of their thermal back-reactions. Such correlative models would aid in the future design of indigo photoswitches with desired properties. To capture the electronic and steric properties of the *N*-aryl groups, we decided to carry out DFT featurization by using the corresponding benzoic acids as computationally low-cost yet effective surrogates (Figure 4). The parameters of the substituted benzoic acids were then extracted and implemented as descriptors in multivariate linear regression models. This modern version of linear free energy analysis (Hammett plot)[21] was recently pioneered by the Sigman group for structure-reactivity/selectivity correlation in various catalytic reactions.[22] However, to the best of our knowledge, this simple while powerful methodology has yet to be applied to the area of photoswitches.[23]

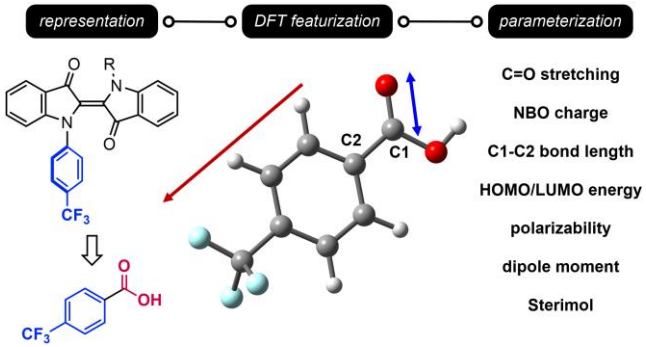

Figure 4. Workflow for correlating the *N*-aryl structures and rate of thermal back-reaction.

We initially tested this workflow on our previously developed *N,N´*-diarylindigos. In addition to the *para*-substituted arenes, five new *meta*-derivatives were included to test the generality (see SI for the complete list of investigated compounds). The benzoic acid surrogate of each aryl group was computed by DFT, and the relevant parameters were tabulated. Specifically, the natural bond orbital (NBO) of C1 and C2 carbons, C=O stretching frequency and intensity, dipole moments, polarizability, as well as HOMO/LUMO energies were applied as inputs to construct linear regression models. When we limited the selection to only two variables, a very high correlation (R^2>0.90) could be obtained with various parameters. For example, by utilizing the C=O stretching frequency of one arene (**Ar¹_ν_C=O**) and the LUMO energy of the other (**Ar²_LUMO**), R^2=0.95 was observed with this dataset, along with Q^2=0.91 for the leave-one-out (LOO) validation (Figure 5a). It is not surprising that multiple combinations are able to provide outstanding correlations as these descriptors are interrelated to each other through their connection to the electronic properties of the arenes. Importantly, the fact that both *para*- and *meta*-series can be included in a single model demonstrates the encouraging generality of this approach.

Subsequently, we turned our attention to the dataset containing our novel *N*-aryl-*N´*-alkylindigos developed in this work. Their structural diversity, both sterically and electronically, potentially poses a challenge to developing a suitable model for capturing all these variations. Following the same workflow, we additionally performed a conformational search to identify the lowest energy structures prior to parameter extraction. Furthermore, we expanded the parameter selection to better accommodate the structure variations. Thus, with four descriptors, excellent levels of correlation were obtained (R^2>0.85). Among all descriptors, C1–C2 bond length (**L_C1-C2**) and NBO charge of C2 (**Ar_NBO_C2**) appear crucial in every single of the outperforming models

(see SI for more details). For instance, along with the LUMO energy (**LUMO**) and the NBO charge of the carbonyl oxygen (**Ar_NBO_=O**), a correlation of R^2=0.89 (Q^2=0.75 for LOO) could be obtained (Figure 5b). When the same model was applied to the rates of thermal back-reaction in toluene, a good level of correlation was observed (see SI for details). Notably, in contrast to the electronic parameters, steric descriptors, i.e., Sterimol values, do not contribute significantly, suggesting that for these compounds, electronic effects imposed by *N*-aryl substituents dominate the rate of their thermal back-reaction.

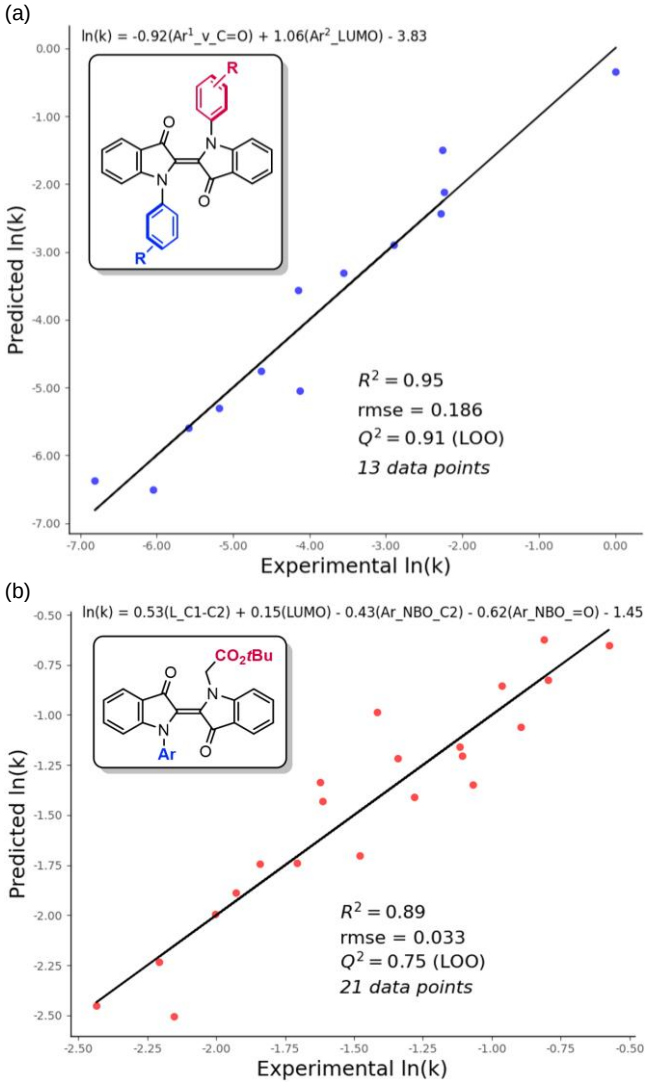

Figure 5. Multivariate regression models for thermal back-reaction rates (k) of (a) *N*,*N*´-diarylindigos (R = *p*-OMe, H, *p*-F, *p*-CF_3, *p*-CN, *p*-NO_2, *m*-OMe, *m*-CHO, *m*-CF_3, *m*-CN, *m*-NO_2) and (b) *N*-aryl-*N*´-alkylindigos (**3a**-**3u**).

This general data-science workflow consisting of structural representation, DFT featurization/parametrization, and construction of multivariate linear regression models is unequivocally demonstrated successful here for correlating the rate of thermal back-reaction of the *N*-aryl indigos. In our opinion, the key to success is the ability to quantitatively describe the electronic properties of *N*-aryl substituents using measurable parameters. As an example, electron-donating groups result in stronger C1–C2 bonds as well as weaker C1=O bonds in the benzoic acid surrogates, which are reflected by their shorter C1–C2 bond length (**L_C1-C2**) and lower C1=O stretching frequency (**Ar_v_C=O**). Another additional advantage of this strategy is that it eliminates the need to perform calculations on the entire indigo structure or any transition state species, thus bypassing tedious and expensive computation process. We expect this approach to be generalizable to other families of molecular photoswitches, in which the main photochromic core is conserved and only peripheral substituents are varied.

CONCLUSION

In this work combining metal catalysis, photochemistry, computation, and data science, we developed a synthetic method for preparing functionalized *N*-arylindigo photoswitches as well as quantitative models to correlate their structures and thermal half-lives. A copper-catalyzed *N*-arylation of indigo dye was achieved using inexpensive reagents to afford a wide array of synthetically useful functional groups. Moreover, this method is completely selective for mono-*N*-arylation despite the presence of a second indigo nitrogen. Computational studies suggest that the selectivity originates from a bimetallic cooperative mechanism, where a binuclear copper-indigo complex is responsible for lowering the overall reaction barrier.

By using this methodology, a collection of functional *N*-aryl-*N*´-alkylindigos containing *N*-aryl substituents of varying electronic and steric properties was prepared. All compounds underwent efficient red-light-triggered photoisomerization, and the thermal half-lives of *Z*-isomers can be modulated by the structures of *N*-aryl groups. A proof-of-concept experiment demonstrated that the *N*´-alkyl groups can be utilized to attach functional moieties without changing the photochromic properties. A data-science workflow including representation, DFT featurization, and parametrization was carried out, where the molecular parameters extracted from computational outcomes were utilized to yield multivariate linear regression models with high level of correlativity. This approach thus represents a bridge for connecting the structures of indigo photoswitches with their thermal half-lives, which is an essential property for future applications. Beyond indigo photoswitches, we expect that this simple workflow can be generalized to correlative modelling of other types of photoresponsive molecules. Further efforts to explore these new functional indigo photoswitches in various biomedical and material science applications are currently underway.

ASSOCIATED CONTENT

The Supporting Information is available free of charge via the Internet at http://pubs.acs.org.

Experimental details including synthetic procedures, compound characterization data, and photochemical and

kinetic experiments, computational and modelling procedures and results (PDF)
Crystallographic data (CIF)

AUTHOR INFORMATION

Corresponding Author

Satoshi Maeda – *Institute for Chemical Reaction Design and Discovery (WPI-ICReDD), Hokkaido University, Sapporo 001-0021, Japan; Department of Chemistry, Faculty of Science, Hokkaido University, Sapporo 060-8628, Japan; orcid.org/0000-0001-8822-1147;* Email: smaeda@eis.hokudai.ac.jp

Stefan Hecht – *DWI-Leibniz Institute for Interactive Materials, 52074 Aachen, Germany; Institute of Technical and Macromolecular Chemistry, RWTH Aachen University, 52074 Aachen, Germany; Department of Chemistry and Center for the Science of Materials Berlin, Humboldt-Universität zu Berlin, 12489 Berlin, Germany;* orcid.org/0000-0002-6124-0222; Email: sh@chemie.hu-berlin.de

Chung-Yang (Dennis) Huang – *Institute for Chemical Reaction Design and Discovery (WPI-ICReDD), Hokkaido University, Sapporo 001-0021, Japan;* orcid.org/ 0000-0003-2618-9668; Email: dcyhuang@icredd.hokudai.ac.jp

Authors

Amit K. Jaiswal – *Institute for Chemical Reaction Design and Discovery (WPI-ICReDD), Hokkaido University, Sapporo 001-0021, Japan*

Priya Saha – *Institute for Chemical Reaction Design and Discovery (WPI-ICReDD), Hokkaido University, Sapporo 001-0021, Japan*

Julong Jiang – *Department of Chemistry, Faculty of Science, Hokkaido University, Sapporo 060-8628, Japan*

Kimichi Suzuki – *Department of Chemistry, Faculty of Science, Hokkaido University, Sapporo 060-8628, Japan*

Anna Jasny – *DWI-Leibniz Institute for Interactive Materials, 52074 Aachen, Germany; Institute of Technical and Macromolecular Chemistry, RWTH Aachen University, 52074 Aachen, Germany*

Bernd M. Schmidt – *Institute for Organic Chemistry and Macromolecular Chemistry, Faculty of Mathematics and Natural Sciences, Heinrich Heine University Düsseldorf, Universitätsstraße 1, 40225 Düsseldorf, Germany;* orcid.org/0000-0003-3622-8106

Notes

The authors declare no competing financial interest.

ACKNOWLEDGMENT

C.-Y. H. is grateful for the financial support provided by the Institute for Chemical Reaction Design and Discovery (WPI-ICReDD) and Hokkaido University as well as the Japan Society for the Promotion of Science (JP22K20522). Moreover, funding by the Deutsche Forschungsgemeinschaft (DFG via SFB 1349, project ID: 387284271) is gratefully acknowledged. S.H. thanks the Einstein Foundation Berlin as well as Humboldt University for generous support. B.M.S. acknowledges the support from the Deutsche Forschungsgemeinschaft SCHM 3101/6-1 (DFG, German Re-search Foundation) and The Center for Structural Studies (DFG Grant number 417919780 and INST 208/740-1 FUGG). We thank Kai Sun for performing reproducibility check of this synthetic methodology.

REFERENCES

(1) (a) Bouas-Laurent, H.; Dürr, H. Organic Photochromism (IUPAC Technical Report). *Pure Appl. Chem.* **2001**, *73*, 639–665. (b) Wang, L.; Li, Q. Photochromism into Nanosystems: Towards Lighting up the Future Nanoworld. *Chem. Soc. Rev.* **2018**, *47*, 1044–1097.

(2) (a) Szymánski, W.; Beierle, J. M.; Kistemaker, H. A. V; Velema, W. A.; Feringa, B. L. Reversible Photocontrol of Biological Systems by the Incorporation of Molecular Photoswitches. *Chem. Rev.* **2013**, *113*, 6114–6178. (b) Velema, W. A.; Szymański, W.; Feringa, B. L. Photopharmacology: Beyond Proof of Principle. *J. Am. Chem. Soc.* **2014**, *136*, 2178–2191. (c) Broichhagen, J.; Frank, J. A.; Trauner, D. A Roadmap to Success in Photopharmacology. *Acc. Chem. Res.* **2015**, *48*, 1947–1960. (d) Hüll, K.; Morstein, J.; Trauner, D. In Vivo Photopharmacology. *Chem. Rev.* **2018**, *118*, 10710–10747.

(3) (a) Zhang, J.; Zou, Q.; Tian, H. Photochromic Materials: More Than Meets The Eye. *Adv. Mater.* **2013**, *25*, 378–399. (b) Goulet-Hanssens, A.; Eisenreich, F.; Hecht, S. Enlightening Materials with Photoswitches. *Adv. Mater.* **2020**, *32*, 1905966.

(4) Zhang, Z.; Wang, W.; O'Hagan, M.; Dai, J.; Zhang, J.; Tian, H. Stepping Out of the Blue: From Visible to Near-IR Triggered Photoswitches. *Angew. Chem. Int. Ed.* **2022**, *61*, e202205758.

(5) Pansare, V. J.; Hejazi, S.; Faenza, W. J.; Prud'homme, R. K. Review of Long-Wavelength Optical and NIR Imaging Materials: Contrast Agents, Fluorophores, and Multifunctional Nano Carriers. *Chem. Mater.* **2012**, *24*, 812–827.

(6) (a) Huang, C.-Y.; Hecht, S. A Blueprint for Transforming Indigos to Photoresponsive Molecular Tools. *Chem. Eur. J.* **2023**, *29*, e202300981. (b) Kaplan, G.; Seferoğlu, Z.; Berdnikova, D. V. Photochromic derivatives of indigo: historical overview of development, challenges and applications. *Beilstein J. Org. Chem.* **2024**, *20*, 228–242.

(7) (a) Brode, W. R.; Pearson, E. G.; Wyman, G. M. The Relation between the Absorption Spectra and the Chemical Constitution of Dyes. XXVII. cis-trans Isomerism and Hydrogen Bonding in Indigo Dyes. *J. Am. Chem. Soc.* **1954**, *76*, 1034–1036. (b) Weinstein, J.; Wyman, G. M. Spectroscopic Studies on Dyes. 11. The Structure of *N,N'*-Dimethylindigo. *J. Am. Chem. Soc.* **1956**, *78*, 4007–4010.

(8) (a) Aiken, S.; Edgar, R. J. L.; Gabbutt, C. D.; Heron, B. M.; Hobson, P. A. Negatively photochromic organic compounds: Exploring the dark side. *Dyes Pigm.* **2018**, *149*, 92–121. (b) Li, R.; Mou, B.; Yamada, M.; Li, W.; Nakashima, T.; Kawai, T. From Visible to Near–Infrared Light–Triggered Photochromism: Negative Photochromism. *Molecules* **2024**, *29*, 155–179.

(9) (a) Ferber, K. H. Toxicology of indigo. A review. *J. Environ. Pathol. Toxicol. Oncol.* **1987**, *7*, 73–83. (b) Steingruber, E. Indigo and Indigo Colorants. Ullmann's Encyclopedia of Industrial Chemistry. Weinheim: Wiley-VCH, 2004.

(10) (a) Pina, J.; Sarmento, D.; Accoto, M.; Gentili, P. L.; Vaccaro, L.; Galvão, A.; de Melo, J. S. S. Excited-State Proton Transfer in Indigo. *J. Phys. Chem. B* **2017**, *121*, 2308–2318. (b) Roy, P. P.; Shee, J.; Arsenault, E. A.; Yoneda, Y.; Feuling, K.; Head-Gordon, M.; Fleming, G. R. Solvent Mediated Excited State Proton Transfer in Indigo Carmine. *J. Phys. Chem. Lett.* **2020**, *11*, 4156–4162.

(11) Huang, C.-Y.; Bonasera, A.; Hristov, L.; Garmshausen, Y.; Schmidt, B. M.; Jacquemin, D.; Hecht, S. *N,N'*-Disubstituted Indigos as Readily Available Red-Light Photoswitches with Tunable Thermal Half-Lives. *J. Am. Chem. Soc.* **2017**, *139*, 15205–15211.

(12) Budzák, Š.; Jovaišaitė, J.; Huang, C.-Y.; Baronas, P.; Tulaitė, K.; Juršėnas, S.; Jacquemin, D.; Hecht, S. Mechanistic Insights into the Photoisomerization of *N,N'*-Disubstituted Indigos. *Chem. Eur. J.* **2022**, *28*, e202200496.

(13) Kuntze, K.; Viljakka, J.; Virkki, M.; Huang, C.-Y.; Hecht, S.; Priimagi, A. Red-light photoswitching of indigos in polymer thin films. *Chem. Sci.* **2023**, *14*, 2482–2488.

(14) (a) van Alphen, J. On Indigo. III. The reaction between indigo, aromatic iodides and potassium carbonate. *Rec. Trav. Chim.* **1938**, *57*, 915–920. (b) Matsumoto, Y.; Tanaka, H. A Simple Preparative Method of *N*-Arrlindigos and Substitution Effect in UV/Visible

Absorption *Heterocycles* **2003**, *60*, 1805–1810. (c) Kim, I. K.; Li, X.; Ullah, M.; Shaw, P. E.; Wawrzinek, R.; Namdas, E. B.; Lo, S.-C. High-Performance, Fullerene-Free Organic Photodiodes Based on a Solution-Processable Indigo. *Adv. Mater.* **2015**, *27*, 6390–6395. (d) Huber, L. A.; Mayer, P.; Dube, H. Photoisomerization of Mono-Arylated Indigo and Water-Induced Acceleration of Thermal *cis*-to-*trans* Isomerization. *ChemPhotoChem* **2018**, *2*, 458–464.

(15) Beletskaya, I. P.; Cheprakov, A. V. The Complementary Competitors: Palladium and Copper in C–N Cross-Coupling Reactions. *Organometallics* **2012**, *31*, 7753–7808.

(16) (a) Tye, J. W.; Weng, Z.; Johns, A. M.; Incarvito, C. D.; Hartwig, J. F. Copper Complexes of Anionic Nitrogen Ligands in the Amidation and Imidation of Aryl Halides. *J. Am. Chem. Soc.* **2008**, *130*, 9971–9983. (b) Strieter, E. R.; Bhayana, B.; Buchwald, S. L. Mechanistic Studies on the Copper-Catalyzed N-Arylation of Amides *J. Am. Chem. Soc.* **2009**, *131*, 78–88. (c) Sung, S.; Sale, D.; Braddock, D. C.; Armstrong, A.; Brennan, C.; Davies, R. P. *ACS Catal.* **2016**, *6*, 3965–3974.

(17) Reviews: (a) Sperotto, E.; van Klink, G. P. M.; van Koten, G.; de Vries, J. G. The mechanism of the modified Ullmann reaction. *Dalton Trans.* **2010**, *39*, 10338–10351. (b) Ribas, X.; Güell, I. Cu(I)/Cu(III) catalytic cycle involved in Ullmann-type cross-coupling reactions. *Pure Appl. Chem.* **2014**, *86*, 345–360. (c) Lo, Q. A.; Sale, D.; Braddock, D, C.; Davies, R. P. *ACS Catal.* **2018**, *8*, 101–109.

(18) (a) Haldón, E.; Álvarez, E.; Nicasio, M. C.; Pérez, P. J. Dinuclear Copper(I) Complexes as Precatalysts in Ullmann and Goldberg Coupling Reactions. *Organometallics* **2009**, *28*, 3815–3821. (b) Jouaiti, A.; Ballerini, L.; Shen, H.-L.; Viel, R.; Polo, F.; Kyritsakas, N.; Haacke, S.; Huang, Y.-T.; Lu, C.-W. Gourlaouen, C.; Su, H.-C.; Mauro, M. Binuclear Copper(I) Complexes for Near-Infrared Light-Emitting Electrochemical Cells. *Angew. Chem. Int. Ed.* **2023**, *62*, e202305569.

(19) Maity, R.; Birenheide, B. S.; Breher, F.; Sarkar, B. Cooperative Effects in Multimetallic Complexes Applied in Catalysis. *ChemCatChem* **2021**, *13*, 2337–2370.

(20) (a) Hein, J. E.; Fokin, V. V. Copper-catalyzed azide–alkyne-cycloaddition (CuAAC) and beyond: new reactivity of copper(I) acetylides. *Chem. Soc. Rev.* **2010**, *39*, 1302–1315. (b) Haldón, E.; Nicasio, M. C.; Pérez, P. J. *Org. Biomol. Chem.* **2015**, *13*, 9528–9550.

(21) (a) Hammett, L. P. The Effect of Structure upon the Reactions of Organic Compounds. Benzene Derivatives. *J. Am. Chem. Soc.* **1937**, *59*, 96–103. (b) Hansch, C.; Leo, A.; Taft, R. W. A survey of Hammett substituent constants and resonance and field parameters. *Chem. Rev.* **1991**, *91*, 165–195.

(22) (a) Santiago, C. B.; Milo, A.; Sigman, M. S. Developing a Modern Approach To Account for Steric Effects in Hammett-Type Correlations. *J. Am. Chem. Soc.* **2016**, *138*, 13424–13430. (b) Santiago, C. B.; Guo, J.-Y.; Sigman, M. S. Predictive and mechanistic multivariate linear regression models for reaction development. *Chem. Sci.* **2018**, *9*, 2398–2412.

(23) Examples of correlating the thermal half-lives of azobenzenes with their structures using machine learning approaches: (a) Griffiths, R.-R.; Greenfield, J. L.; Thawani, A. R.; Jamasb, A. R.; Moss, H. B.; Bourached, A.; Jones, P.; McCorkindale, W.; Aldrick, A. A.; Fuchter, M. J.; Lee, A. A. Data-driven discovery of molecular photoswitches with multioutput Gaussian processes. *Chem. Sci.* **2022**, *13*, 13541–13551. (b) Axelrod, S.; Shakhnovich, E.; Gómez-Bombarelli, R. Thermal Half-Lives of Azobenzene Derivatives: Virtual Screening Based on Intersystem Crossing Using a Machine Learning Potential. *ACS Cent. Sci.* **2023**, *9*, 166–176.

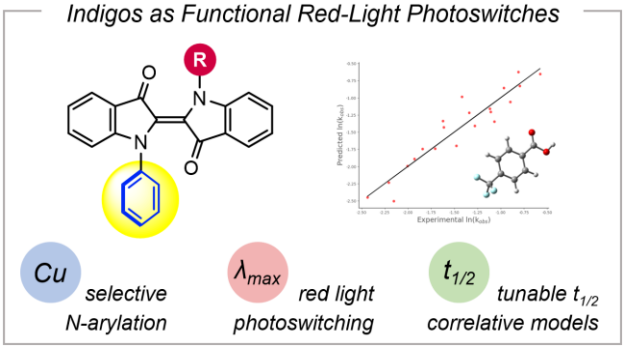

TOC